Chemical Engineering Science 64 (2009) 4758 – 4764

Contents lists available at ScienceDirect

Chemical Engineering Science

journal homepage: www.elsevier.com/locate/ces

The experimental observation and modelling of microdroplet formation within a plastic microcapillary array

Bart Hallmark, Chirag Parmar, David Walker, Christian H. Hornung, Malcolm R. Mackley*, John F. Davidson

Department of Chemical Engineering and Biotechnology, New Museums Site, Pembroke Street, Cambridge CB2 3RA, UK

ARTICLE INFO

Article history:
Received 12 August 2008
Received in revised form 15 April 2009
Accepted 20 April 2009
Available online 3 May 2009

Keywords:
Droplet generation
Fluid mechanics
Laminar flow
Mathematical modelling
Microfluidics
Multiphase flow

ABSTRACT

This paper reports an experimental study of the formation of a two-phase liquid mixture in a circular capillary tube of 0.74 mm diameter. Organic liquid, the continuous phase, flowed through the capillary. Aqueous liquid, the dispersed phase, was injected through a hypodermic entering the side of the capillary and a stream of aqueous droplets was formed in the flowing organic liquid. The observed droplet diameters depended strongly on the ratio of the flow-rates between the dispersed and continuous phases: droplet diameters ranged between 480 and 64 μm. A simple model gave good predictions, matching the data and showing how the droplet diameter is dependant on the flow rates of the two phases. The flow geometry was similar to the T-junction configuration used for emulsion formation in microfluidic devices and was fabricated from an extruded plastic capillary array termed a microcapillary film (MCF).

1. Introduction and background

The generation of small drops and emulsions where the dispersed phase has a very low degree of polydispersity has received attention in recent years. Early work (Umbanhowar et al., 2000) used a selection of very fine glass capillaries with internal diameters ranging between 0.7 and 100 μm to introduce an aqueous phase into a shear flow of organic phase containing a small amount of surfactant. Under carefully controlled conditions, the flow field of the organic phase around the tip of the glass capillary caused the aqueous phase to break off in a periodic fashion creating an emulsion. This emulsion contained effectively monodisperse droplets, with droplet diameters ranging between 2 and 200 μm.

The ability to fabricate geometries containing rectangular-sectioned microchannels paved the way for a large body of research investigating the creation of two-phase or multi-phase flows in microfluidic devices. Early fabrication techniques consisted typically of milled quartz or etched Pyrex plates (Okushima et al., 2004), slit-saw cut soda lime glass (Burns and Ramshaw, 2001), the creation of positive moulds in materials such as silicon via photolithography prior to moulding in acrylated urethanes (Thorsen et al., 2001), micromoulding and laser ablation (Beebe et al., 2002). More recently, the most common choice of fabrication technique appears to be the use of soft lithography to create a geometry in a soft polymer such as poly-dimethylsiloxane (PDMS) (Zheng et al., 2003; Song and Ismagilov, 2003; Garstecki et al., 2004; Song et al., 2003). A variety of different microfluidic geometries have been investigated, ranging from passive (Okushima et al., 2004; Thorsen et al., 2001) or active (Willaime et al., 2006) 'T'-junction style devices, cross geometries (Burns and Ramshaw, 2001; Dreyfus et al., 2003; Cubaud and Ho, 2004) and flow focusing devices (Ganan-Calvo and Gordillo, 2001; Garstecki et al., 2004; Raven et al., 2006) through to more elaborate geometries containing multiple flow branches (Link et al., 2004) and terrace-and-well style geometries (Sugiura et al., 2001).

A universally recorded result from research in this field is the ability to generate dispersed phases with a very low degree of polydispersity, independent of whether the dispersed phase was a gas in a continuous liquid phase (Burns and Ramshaw, 2001; Cubaud and Ho, 2004; Ganan-Calvo and Gordillo, 2001; Garstecki et al., 2004; Raven et al., 2006), or whether the dispersed phase was an aqueous phase in an organic phase (Link et al., 2004; Song and Ismagilov, 2003; Song et al., 2003; Thorsen et al., 2001). Elaborate gaseous dispersed phase structures have also been observed and mapped (Cubaud and Ho, 2004; Raven et al., 2006; Thorsen et al., 2001) and conditions discovered where it is possible to encapsulate multiple aqueous phase droplets within a single organic droplet (Okushima et al., 2004) or bring together multiple aqueous phases forming a single droplet of an aqueous mixture within an organic disperse phase (Tice et al., 2003).

Applications for microfluidic devices that can generate a dispersed phase with a low degree of polydispersity are potentially widespread. The ability to generate accurately sized monodisperse emulsions has interesting application, for example, in optics for the generation of liquid-crystal interference-based electro-optic phase

* Corresponding author.
E-mail address: mrm5@cam.ac.uk (M.R. Mackley).

0009-2509/$ - see front matter © 2009 Elsevier Ltd. All rights reserved.
doi:10.1016/j.ces.2009.04.027

Fig. 1. Photomicrograph of the cross section of a microcapillary film (MCF) extruded in linear low-density polyethylene (LLDPE).

gratings (Rudhardt et al., 2003). In addition, the circulation patterns present within the disperse phase (Burns and Ramshaw, 2001; Song and Ismagilov, 2003; Song et al., 2003), coupled with the nanolitre volume of fluid required for droplet formation, allow for highly accurate measurement of reaction kinetics in chemical and biochemical systems (Song and Ismagilov, 2003; Song et al., 2003). A key feature of using the disperse phase as a series of miniature chemical reactors is that dispersion of the reagents along the length of the microchannel is suppressed due to the immiscibility of the reacting phase in the continuous phase (Song and Ismagilov, 2003; Song et al., 2003).

This paper presents initial results from research to investigate whether it is possible to form a dispersed phase of aqueous microdroplets in an organic continuous phase within a novel, extruded, plastic capillary array. The array that was used is termed a microcapillary film (MCF) (Hallmark et al., 2005a,b), which consists of an array of 19 equispaced capillaries that run along the length of a plastic film; a photomicrograph of a typical MCF cross section is shown in Fig. 1.

MCFs have a number of useful features for droplet generation when compared with conventional materials used for microfluidic geometries. The first of these is cost; MCFs are extrusion processed which, in principle, means that their unit cost could be of a similar order of magnitude to plastic bags; the eventual price depends on the polymer from which MCFs are extruded. MCFs have been successfully extruded from a variety of polymers including polyethylene and polypropylene, but they can also be made from high-performance fluoropolymers. The exceptional temperature and solvent resilience of these fluoropolymer materials would allow droplet formation in temperature and solvent environments where many of the current low-cost materials such as PDMS or moulded acrylated urethanes would fail. High temperatures and excellent solvent tolerance are features of glass-based systems, but fabrication of microfluidic devices in these materials is likely to be more expensive than fluoropolymer MCF. A consequence of low unit cost is the ability to create disposable systems such that stringent purity standards can be achieved and contamination avoided. Previous research has explored the hydrodynamic response and heat transfer performance of MCFs (Hornung et al., 2006) along with proof-of-concept studies where MCFs have been used as chemical microreactors (Hornung et al., 2007).

2. Experimental apparatus and protocol

A 1 m length of MCF was used that contained an array of 19 capillaries with mean hydraulic diameter 740 μm, extruded in-house from Dow Affinity® polyolefin plastomer. This material was chosen because it has good optical clarity and is pliable enough to allow a flat-tipped, three-quarter inch long 36-gauge hypodermic needle (Coopers Needle Works Ltd., Birmingham, UK) to be inserted through the side of MCF into a capillary; the Affinity® plastomer also sealed acceptably around the inserted needle, preventing significant leakage. The outlet end of the needle was usually on, or near, the centreline of the capillary, see Figs. 2 and 3(B) and (C); sometimes, however, the outlet was near the capillary wall, see Fig. 3(A). It was perceived that the position of the needle had only a second order effect on droplet formation. The internal diameter of the needle was 101 μm. The length between the needle insertion point and the open end of the MCF was initially set to 0.852 m. Sunflower oil containing 10% by volume surfactant (washing up liquid) was used as the continuous organic phase; this was injected into a capillary using a syringe pump (Sage Instruments, Model 355). The aqueous phase consisted of distilled water containing red food colouring and was contained in a reservoir whose height above the injection point in the MCF could be adjusted. The aqueous phase entered through the above-mentioned hypodermic needle inserted into the MCF. Observation of the flow patterns within the MCF was via an optical microscope with an inbuilt CCD video camera (Intel QX3). A schematic diagram of the apparatus is shown in Fig. 2.

Preliminary studies found that it was possible to create elongated or spherical droplets as the dispersed phase within the MCF-based system, and that the form of the disperse phase, whether spherical droplets or elongated slugs, depended on the aqueous phase to organic phase flow-rate ratio. It was further found that parallel production of microdrops was possible by using multiple capillaries, each with its own injector. The photomicrographs shown in Fig. 3 give examples of the form of the disperse phase and also of droplet formation in parallel. The elongated droplets, Fig. 3(A), will be described as 'slugs'.

The experimental protocol was designed to map out the behaviour of the dispersed phase over a wide range of aqueous phase to organic phase flow-rate ratios. Variation of the organic phase flow-rate, Q_o, was achieved *via* control of the syringe pump piston speed, whereas variation of the aqueous phase flow-rate was achieved by changing the height, h, of the aqueous phase reservoir; see Fig. 4. Manipulation of the length, L_o, of the MCF downstream of the aqueous phase injection point also changed the aqueous phase flow-rate by changing the gauge pressure, ΔP, at the point of injection; see Fig. 4. Both methods of aqueous phase flow-rate control, i.e., varying h and ΔP, were used; the nature of the pressure balance at the point of injection is explored below.

The experimental protocol consisted of a series of 'nested' studies. Initially, the aqueous phase reservoir head height, h, was set at 1 m to establish an aqueous phase flow-rate, Q_a, at the lowest value of the organic phase flow rate, Q_o, that could be supplied by the syringe pump ($0.057\,\mathrm{mm^3\,s^{-1}}$). Once both flows had had sufficient time to reach steady-state, typically about 5 min, a series of video sequences showing the flow pattern within the capillary was captured using the microscope. The organic phase flow rate was then increased, the flows were allowed to stabilise and more images acquired. During the course of observation, the head height, h, was observed to remain essentially constant.

This procedure was repeated until Q_o became too high, and droplet formation ceased. When this condition had been met, the aqueous phase reservoir was lowered by 10 cm, Q_o was reduced to its minimum value and the protocol of capturing images at different organic phase flow-rates repeated for the new Q_a. Up to eight different values of h were used, with the experiment terminating when h became too small for droplet formation.

Once droplet formation had ceased at the combination of the lowest Q_a and highest Q_o, a short length (roughly 10 cm) of MCF downstream of the aqueous phase injection point was cut off. The new distance between the aqueous phase injection point and the end of the MCF was then measured. The removal of a short piece of MCF had the effect of decreasing ΔP, thus increasing the aqueous phase flow-rate for given h. With the shorter MCF, h was returned to its initial value, Q_o returned to its lowest value and sequences of images captured for increasing Q_o at given Q_a as before. Eight different lengths, L_o, of MCF were used, the shortest being 0.270 m. Throughout this protocol, the MCF was kept horizontal. The experimental protocol is illustrated schematically in Fig. 5.

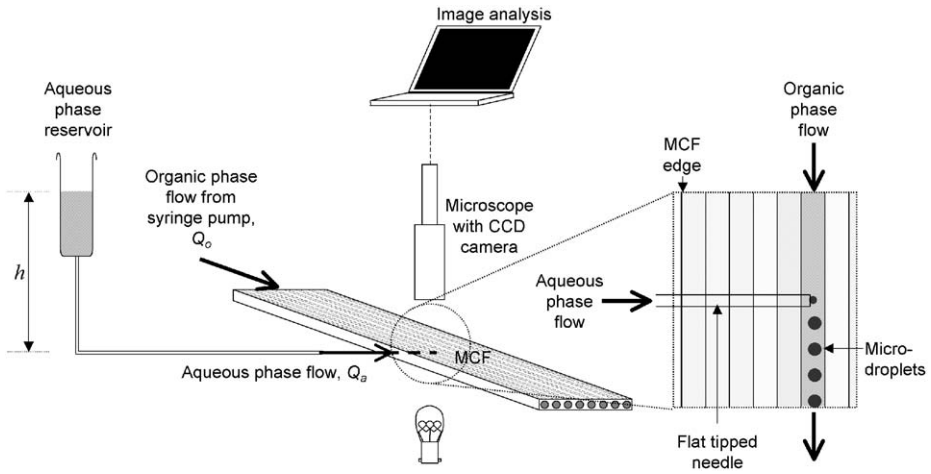

Fig. 2. Schematic diagram of the experimental equipment used to generate microdrops.

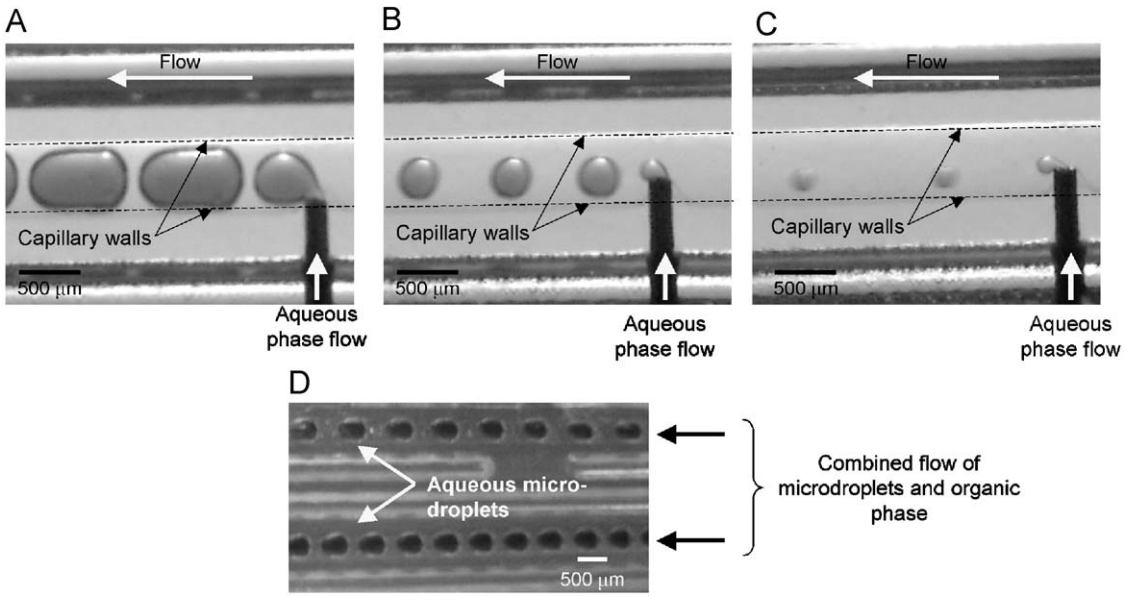

Fig. 3. Photomicrographs illustrating: (A) microslug formation at high aqueous phase flow rates and low organic phase flow rates, (B) medium-size microdroplet formation at comparable organic and aqueous phase flow rates and (C) formation of small microdrops at high organic phase flow rates and low aqueous phase flow rates. Also shown in (D) is a proof-of-concept for simultaneous microdroplet formation in multiple capillaries.

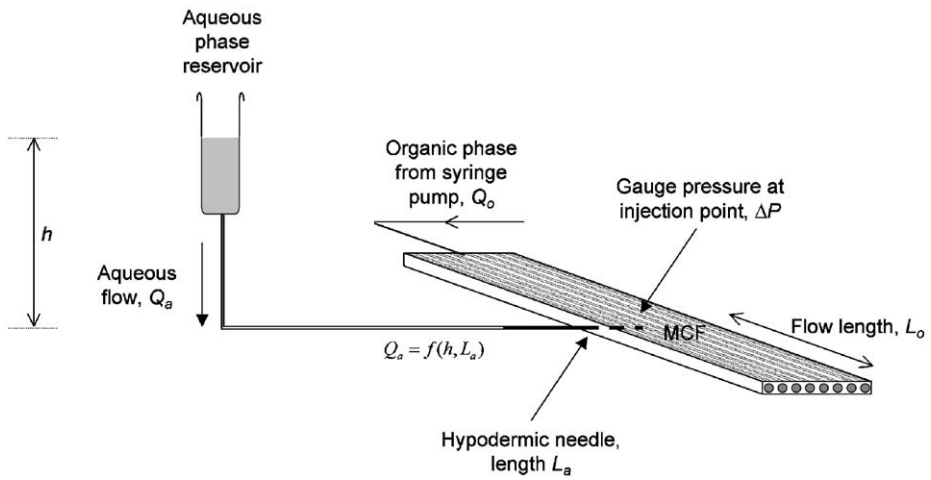

Fig. 4. Schematic diagram illustrating the dependent variables controlling the aqueous phase flow-rate.

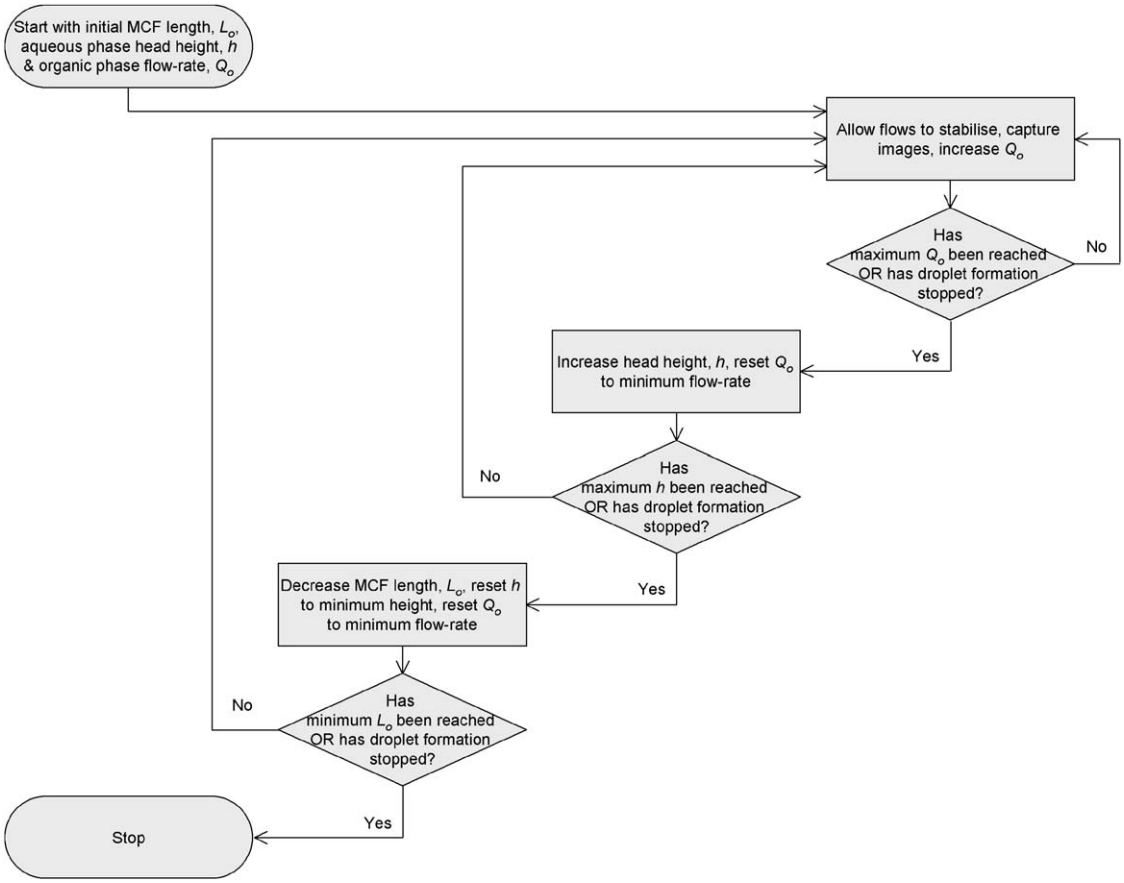

Fig. 5. Flow chart illustrating the 'nested' structure of the experimental protocol.

3. Results

Using the experimental protocol outlined above, it was possible to create an aqueous disperse phase within a continuous organic phase. In each case, the aqueous phase reservoir head height, h, was used to calculate the aqueous phase flow-rate; this calculation is given in the modelling section that follows. The form of the disperse phase depended on the relative magnitudes of the flow-rates of the two phases, but typically was either (i) microslugs when the magnitude of the aqueous phase flow-rate was dominant or (ii) droplets when the magnitude of the two-flow rates were comparable or dominated by the organic phase flow-rate. For the spherical droplets, shown in Fig. 3(B), the measurement of diameter is obvious. For the slugs, Fig. 3(A), the diameter was taken as that of the nearly cylindrical section measured normal to the axis of the capillary. Here, the term 'slug' means a droplet formed from a near-cylinder with hemispherical ends, as seen in Fig. 3(A). The trend observed was that the droplet diameter became smaller with increasing organic phase flow-rate.

Image analysis on each set of photographs gave a quantitative measure of droplet diameter as a function of organic and aqueous phase flow rates. These diameter measurements were converted to a percentage of the capillary diameter and plotted as a function of organic and aqueous phase flow rates, see Fig. 6. The organic phase flow rate, Q_o, was obtained from the syringe pump piston speed, as noted above; the aqueous phase flow rate, Q_a, was calculated from the aqueous head, h, together with a term containing Q_o, see Eq. (2).

For clarity, Fig. 6 has been subdivided into a number of zones; (A) represents drops and slugs with a diameter exceeding 97.5% of the capillary diameter, d, (B) represents large droplets with diameters ranging between 67.5% and 97% of d, (C) represents medium droplets with diameters ranging between 47.5% and 67.5% of d, (D) represents small droplets with diameters ranging between 22.5% and 47.5% of d and (E) represents small droplets with diameters less than 22.5% of d, where d was 740 μm. It was not possible to observe droplets smaller than about 8.5% of the capillary diameter, which corresponds to a lower size limit of 64 μm or a volume of 0.14 nL.

4. Modelling droplet size

A number of different models are presented in the literature to predict droplet diameter as a function of the flow-rate of either the continuous or disperse phase. An expression has been derived to calculate the bubble size in a gas–liquid flow-focusing device (Ganan-Calvo and Gordillo, 2001); the characteristic time for bubble formation is predicted by using a pressure balance across the microfluidic geometry and relating this to surface tension and flow effects. Other approaches specific to liquid-phase emulsions (Sugiura et al., 2001) use an energy balance to estimate the interfacial free energy needed to form a droplet and relate this to droplet diameter.

Fig. 7 shows how the aqueous phase was injected, via a hypodermic needle, into one of the capillaries of the MCF, which contained the oil phase. The volume flow rate, Q_o, entering the chosen capillary was determined by the syringe pump, as noted above. The flow rate of aqueous liquid, Q_a, was calculated from the pressure balance given below using the measured head, h, of aqueous phase above the MCF, see Fig. 7.

The gauge pressure, ΔP, at the point where the hypodermic needle entered the MCF was obtained from the Poiseuille equation for

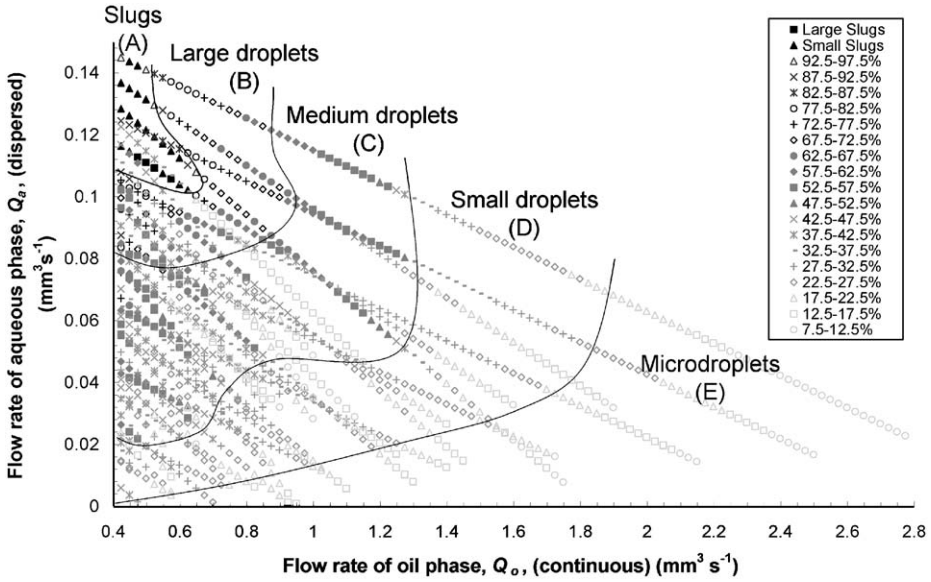

Fig. 6. Plot of droplet diameter expressed as a percentage of capillary diameter as a function of aqueous and organic phase flow rates.

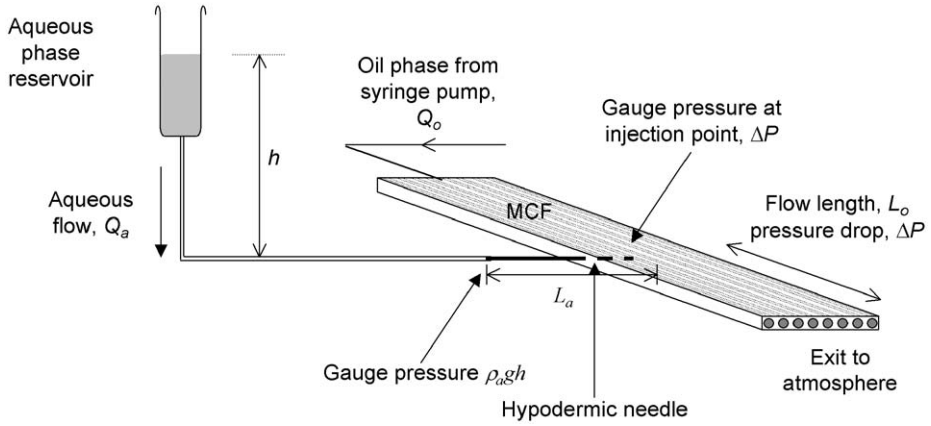

Fig. 7. Schematic diagram of the pressure balance used to calculate the aqueous (disperse) phase flow-rate and the pressure at the tip of the needle that introduces this phase.

laminar flow of oil in the MCF capillary, giving

$$\Delta P = \frac{8Q_o\mu_o L_o}{\pi R_o^4} \tag{1}$$

Here, μ_o is the viscosity of the oil phase, R_o the radius of the MCF capillary, whose flow length is L_o, measured between the point of injection and the MCF exit to atmosphere. The tube conveying the aqueous liquid from the reservoir to the hypodermic was of diameter large enough to give negligible wall friction, and the aqueous velocities were small enough to give negligible energy losses due to bends and junctions. Hence the gauge pressure at entry to the hypodermic was $\rho_a gh$, ρ_a being the density of the aqueous phase and g the acceleration due to gravity; so the pressure difference across the hypodermic was $(\rho_a gh - \Delta P)$, ΔP being given by Eq. (1).

Again using the Poiseuille equation, but for laminar flow of aqueous liquid through the hypodermic needle, gives the volume flow rate

$$Q_a = \frac{\pi R_a^4}{8\mu_a L_a}\left(\rho_a gh - \frac{8Q_o\mu_o L_o}{\pi R_o^4}\right) \tag{2}$$

Here, R_a is the internal radius of the hypodermic needle, whose length is L_a; μ_a is the viscosity of the aqueous phase.

Fig. 8 shows how the aqueous liquid forms droplets as it is injected into the flow of oil through the MCF capillary.

Initially, the growing droplet envelops the tip of the needle from which it receives the aqueous liquid. Assuming the droplet is spherical, its radius r, at time t after initiation, is given by

$$Q_a t = \frac{4\pi r^3}{3} \tag{3}$$

Thus the radius is proportional to $t^{1/3}$, so the droplet grows rapidly for small t, because $dr/dt \propto 1/t^{2/3}$; hence the droplet continues to envelop the end of the needle. However, the flow of oil moves the droplet, so its upstream surface must eventually cross the end of the needle, when the droplet detaches.

There are two alternative assumptions about detachment, as follows:

(1) The droplet is assumed to detach when the upstream surface reaches the centreline of the needle, i.e., when

$$x = U_c t = r \tag{4}$$

x being the distance travelled by the centre of the droplet, which is assumed to move with the velocity, U_c, of the oil on the

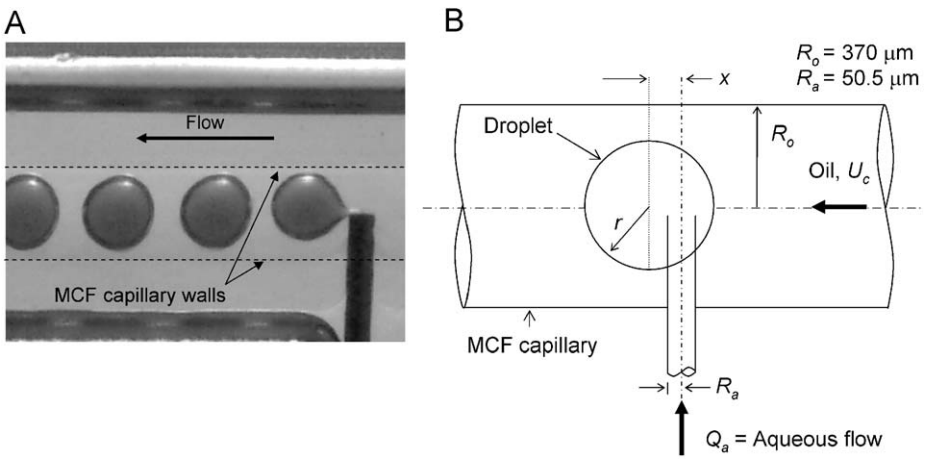

Fig. 8. (A) Photomicrograph of droplet formation, illustrating the typical manner in which drops detach from the injecting needle and (B) schematic diagram illustrating theoretical droplet growth and motion away from the injecting needle during formation.

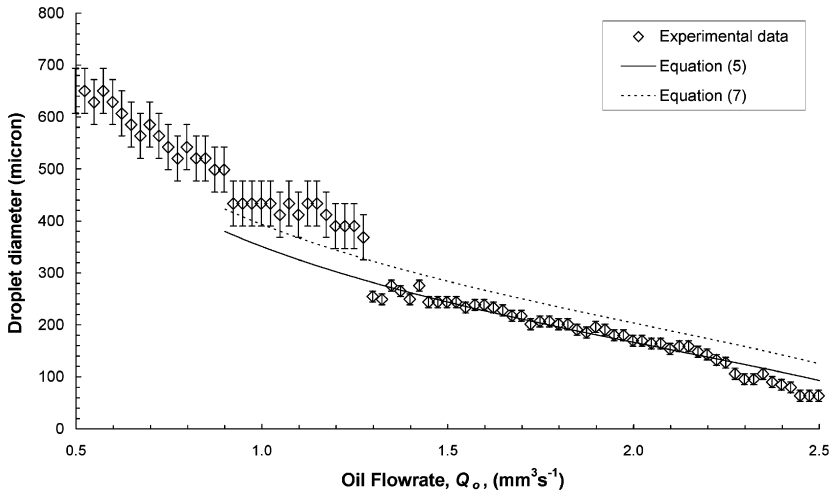

Fig. 9. Plot of the observed experimental droplet diameter (open diamonds) as a function of organic phase flow rate. The theoretical curves used Eq. (2) to get Q_a and r_d from Eqs. (5) and (7), with $U_c = 2Q_o/\pi R_o^2$. Values used: $R_a = 50.5\,\mu m$, $R_o = 370\,\mu m$, $L_a = 19.1\,mm$, $L_o = 0.27\,m$, $h = 0.718\,m$, $\mu_a = 0.001\,Pa\,s$, $\mu_o = 0.067\,Pa\,s$ and $\rho_a = 994\,kg\,m^{-3}$.

centreline of the MCF capillary. Eliminating t from Eqs. (3) and (4) gives the radius at detachment

$$r_d = \sqrt{\frac{3Q_a}{4\pi U_c}} \tag{5}$$

(2) Alternatively, the droplet is assumed to detach when the upstream surface reaches the downstream side of the needle, i.e., when

$$x = U_c t = R_a + r_d \tag{6}$$

Eliminating t from Eqs. (3) and (6) gives an expression from which to obtain r_d:

$$\frac{4\pi r_d^3 U_c}{3Q_a} = R_a + r_d \tag{7}$$

Eq. (7), a cubic in r, gives larger values of r than Eq. (5).

Fig. 9 shows one set of measurements of droplet diameter as a function of volumetric flow rate, where the MCF length, L_o, is 0.270 m and the aqueous phase reservoir height, h, is 0.718 m. The error bars in this plot are calculated from uncertainty in droplet diameter due to refraction effects. Also shown in Fig. 9 are the two theoretical predictions from Eqs. (5) and (7) representing the two assumptions about droplet detachment i.e., (1) at the centreline of the injection needle and (2) at the downstream wall of the needle.

The plot shown in Fig. 9 demonstrates that, despite the simple nature of the models, the overall trend of the experimental data is captured and a quantitative match between experimental data and Eq. (5) is obtained between $Q_o = 1.3$ and $2.5\,mm^3\,s^{-1}$. Eq. (5) tends to perform better at organic phase flow rates above roughly $1.3\,mm^3\,s^{-1}$, whereas Eq. (7) performs better at organic phase flow rates under $1.3\,mm^3\,s^{-1}$. The relative merits of each model can be attributed to the nature of the drops and the manner in which they were observed to detach. At low organic phase flow rates, the drops were typically microslugs, so the validity of some of the assumptions in the analysis is questionable, particularly the hypothesis that each droplet is spherical during formation. At the higher organic phase flow rates, where the experimental data and Eq. (5) match, the disperse phase was observed to take the form of spherical microdroplets, hence satisfying the assumptions in the analysis.

In terms of accounting for the detachment point of the droplet from the injecting needle, it can be seen from Fig. 8(A) that the droplet that has been formed detaches at a point significantly downstream of the centreline of the injecting needle. At this point, a very

thin liquid thread can be seen connecting the droplet to the aqueous phase fluid source. The assumption underlying Eq. (5) was that the droplet detached when its upstream side coincided with the centreline of the injecting needle. Evidently, this is not entirely correct. However, it may be that most of the droplet growth occurs while it envelops the centreline of the needle, and that flow through the liquid thread, formed as the droplet moves away from the needle centreline, is insignificant in relation to the droplet volume.

5. Conclusions

This paper reports successful emulsion generation using a novel, extruded, microfluidic geometry based on a polyolefin plastomer. The form of the disperse phase within the emulsion has been shown to be either microslugs or microdrops, depending on the relative magnitudes of the disperse phase and continuous phase flow rates. The microdroplet diameter ranged between 480 and 64 μm, corresponding to droplet volumes between 58 and 0.14 nL, respectively. A rigorous experimental mapping was carried out to relate the disperse phase flow regime and droplet diameter to the relative magnitudes of the disperse and continuous phase volumetric flow rates.

A simple model is presented that predicts the droplet diameter as a function of the disperse and continuous phase volumetric flow rates. A reasonably accurate match between the predictions of this model and the experimentally determined diameter of the spherical microdrops was obtained.

Based on the research in this paper, MCF-based devices could have great potential for parallel, high throughput, microdroplet formation.

Notation

g	acceleration due to gravity, $\mathrm{m\,s^{-2}}$
h	height of aqueous phase reservoir, m
L_a	length of injecting needle, m
L_o	length of MCF from needle injection to outlet, m
ΔP	gauge pressure in MCF where needle enters capillary, Pa
Q_a	aqueous phase volumetric flow-rate, $\mathrm{m^3\,s^{-1}}$
Q_o	organic phase volumetric flow-rate, $\mathrm{m^3\,s^{-1}}$
r	droplet radius during formation, m
r_d	droplet radius at detachment, m
R_a	injecting needle radius, m
R_c	capillary radius, m
t	time after droplet initiation, s
U_c	centreline velocity of organic phase, $\mathrm{m\,s^{-1}}$
x	distance travelled by centre of droplet, m

Greek letters

μ_a	aqueous phase viscosity, Pa s
μ_o	organic phase viscosity, Pa s
ρ_a	aqueous phase density, $\mathrm{kg\,m^{-3}}$

Acknowledgements

This paper is submitted as part of a Festschrift in honour of Professor Morton Denn. Mort has had close association with two of the authors in this paper, MRM and JFD, and we are delighted to be associated with Professor Denn's many contributions to Chemical Engineering in general and polymer rheology in particular.

The assistance of Cooper's Needleworks Ltd., Birmingham is gratefully acknowledged during the course of this research project. The assistance of the EPSRC is also gratefully acknowledged for funding some of the elements of this research.

References

Beebe, D.J., Mensing, G.A., Walker, G.M., 2002. Physics and applications of microfluidics in biology. Annual Review of Biomedical Engineering 4, 261–286.
Burns, J.R., Ramshaw, C., 2001. The intensification of rapid reactions in multiphase systems using slug flow in capillaries. Lab on a Chip 1, 10–15.
Cubaud, T., Ho, C.M., 2004. Transport of bubbles in square microchannels. Physics of Fluids 16, 4575–4585.
Dreyfus, R., Tabeling, P., Willaime, H., 2003. Ordered and disordered patterns in two-phase flows in microchannels. Physical Review Letters 90, 144505.
Ganan-Calvo, A.M., Gordillo, J.M., 2001. Perfectly monodisperse microbubbling by capillary flow focusing. Physical Review Letters 87, 274501.
Garstecki, P., Gitlin, I., Diluzio, W., Whitesides, G.M., Kumacheva, E., Stone, H.A., 2004. Formation of monodisperse bubbles in a microfluidic flow-focusing device. Applied Physics Letters 85, 2649–2651.
Hallmark, B., Gadala-Maria, F., Mackley, M.R., 2005a. The melt processing of polymer microcapillary film (MCF). Journal of Non-Newtonian Fluid Mechanics 128, 83–98.
Hallmark, B., Mackley, M.R., Gadala-Maria, F., 2005b. Hollow microcapillary arrays in thin plastic films. Advanced Engineering Materials 7, 545–547.
Hornung, C.H., Hallmark, B., Hesketh, R.P., Mackley, M.R., 2006. The fluid flow and heat transfer performance of thermoplastic microcapillary films. Journal of Micromechanics and Microengineering 16, 434–447.
Hornung, C.H., Mackley, M.R., Baxendale, I.R., Ley, S.V., 2007. A microcapillary flow disc reactor for organic synthesis. Organic Process Research and Development 11, 399–405.
Link, D.R., Anna, S.L., Weitz, D.A., Stone, H.A., 2004. Geometrically mediated breakup of drops in microfluidic devices. Physical Review Letters 92, 054503.
Okushima, S., Nisisako, T., Torii, T., Higuchi, T., 2004. Controlled production of monodisperse double emulsions by two-step droplet breakup in microfluidic devices. Langmuir 20, 9905–9908.
Raven, J.P., Marmottant, P., Graner, F., 2006. Dry microfoams: formation and flow in a confined channel. European Physical Journal B: Condensed Matter Physics 51, 137–143.
Rudhardt, D., Fernandez-Nieves, A., Link, D.R., Weitz, D.A., 2003. Phase switching of ordered arrays of liquid crystal emulsions. Applied Physics Letters 82, 2610–2612.
Song, H., Ismagilov, R.F., 2003. Millisecond kinetics on a microfluidic chip using nanoliters of reagents. Journal of the American Chemical Society 125, 14613–14619.
Song, H., Tice, J.D., Ismagilov, R.F., 2003. A microfluidic system for controlling reaction networks in time. Angewandte Chemie 42, 768–772.
Sugiura, S., Nakajima, M., Iwamoto, S., Seki, M., 2001. Interfacial tension driven monodispersed droplet formation from microfabricated channel array. Langmuir 17, 5562–5566.
Thorsen, T., Roberts, R.W., Arnold, F.H., Quake, S.R., 2001. Dynamic pattern formation in a vesicle-generating microfluidic device. Physical Review Letters 86, 4163–4166.
Tice, J.D., Song, H., Lyon, A.D., Ismagilov, R.F., 2003. Formation of droplets and mixing in multiphase microfluidics at low values of the Reynolds and the capillary numbers. Langmuir 19, 9127–9133.
Umbanhowar, P.B., Prasad, V., Weitz, D.A., 2000. Monodisperse emulsion generation via drop break off in a coflowing stream. Langmuir 16, 347–351.
Willaime, H., Barbier, V., Kloul, L., Maine, S., Tabeling, P., 2006. Arnold tongues in a microfluidic drop emitter. Physical Review Letters 96, 054501.
Zheng, B., Roach, L.S., Ismagilov, R.F., 2003. Screening of protein crystallization conditions on a microfluidic chip using nanoliter-size droplets. Journal of the American Chemical Society 125, 11170–11171.